

3. Amundsen-Scott South Pole Station (9/15/21–3/29/22)

This report describes quality control of solar data recorded at Amundsen-Scott South Pole Station between 9/15/21 and 3/29/22. The period resulted in a total of 15,377 solar scans from the SUV-100 spectroradiometer, which were assigned to Volume 31. Because of the ongoing COVID-19 pandemic, the station could not be visited for performing instrument maintenance, which is typically completed on a semi-annual basis. For the same reason, a comparison of the station's on-site standards of spectral irradiance with a traveling standard could not be performed. These restrictions led to slightly increased uncertainties in published solar data. For example, the uncertainty is increased by about 2% between September and December 2021. As in the past, the accuracy of solar data from the SUV-100 system was assured based on comparisons with measurements of the station's GUV-541 radiometer plus results of radiative transfer model calculation. The latter are part of the SUV-100's Version 2 dataset.

Partly because of deferred maintenance due to the COVID-19 pandemic, calibrated solar data are affected by the following issues:

- The consistency of calibration scans was relatively poor; several scans could not be used for the processing of solar data (see Section 3.1) A rigorous comparison of working, long-term, and traveling standards could not be performed.
- The responsivity of the system exhibited a large and unexplained change on 1/15/22.
- The wavelength stability of the SUV-100 monochromator was degraded, requiring frequent adjustment of the system's wavelength registration during post-processing.
- After a "major" upgrade of the Windows 10 Operating System on 1/3/22, communication between the system's control computer and peripheral electronics slowed-down considerably. As a consequence, spectral scans lasted longer than 15 minutes and the standard schedule of four scans per hour could no longer be maintained. On 1/4/22 and 1/5/22, only two scans per hour were executed. On 1/6/22, the schedule was changed to three scans per hour, and from this point onwards, solar measurements start at the top of the hour, and 20 and 40 minutes past the top of the hour. The same issue also started to affect measurements at McMurdo and Palmer when the operating system was updated. As of this writing, there is still no solution available for addressing this problem.

Since 2014, measurements of the 320 nm channel of the GUV-541 radiometer (S/N 29239) that is installed next to the SUV-100 spectroradiometer drifted greatly. GUV data products had to be produced without utilizing measurements of this channel. A comparison of calibrated GUV and SUV data performed during the Volume 26 season indicated that the quality of GUV data products is only marginally affected by the omission of the 320 nm channel. Solar data of the GUV are therefore part of the published datasets.

The system's PSP radiometer was installed during the site visit in January 2020. Its serial number is 27228F3 and it has a calibration factor of $8.332 \times 10^{-6} \text{ V}/(\text{W m}^{-2})$. Data from the systems TUVR radiometer (S/N 27305) were erratic between 1/1/22 and 2/12/22 and were removed from the published datasets.

On 12/4/21, a solar eclipse was visible from Antarctica. At the South Pole, the eclipse started on 6:59:51 and ended on 8:49:34 UT. The eclipse maximum (magnitude of 0.916) occurred on 7:54:43 UT when approximately 95% of the solar disk was covered by the Moon. Figure 3.1 shows measurements of the UV Index by the SUV-100 and GUV-541 radiometers during the eclipse. The two datasets are in good agreement. Note that GUV-541 data have a time resolution of 1 minute while SUV-100 spectra are measured every 15 minutes.

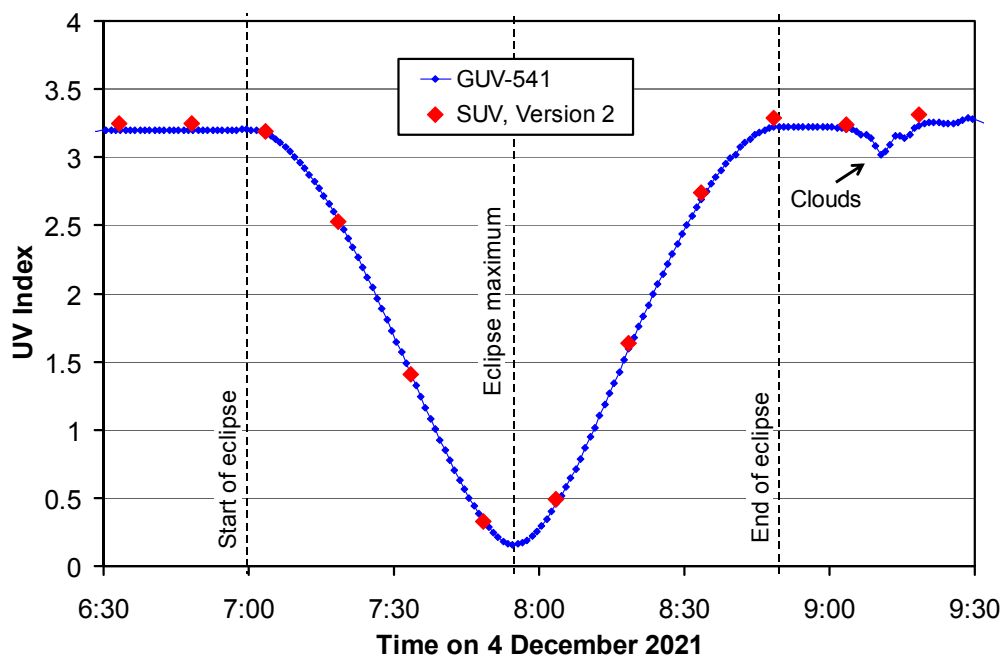


Figure 3.1. UV Index at the South Pole during the solar eclipse of 12/4/21. Measurements by the SUV-100 spectroradiometer (Version 2 data) and GUV-541 radiometer are in good agreement. During the eclipse maximum, the UV Index is about 5% of the value expected from the unobstructed Sun. Measurements were only minimally affected by clouds.

3.1. Irradiance Calibration

The on-site irradiance standards used for calibrating the SUV-100 spectroradiometer during the reporting period were the lamps M-666, 200W021, 200W013, 200WN005 and 200WN006. Lamps M-666, 200W021, and 200W013 are “working standards,” which are used on a regular basis. Please see previous Operations Reports on the history of these lamps. Lamps 200WN005 and 200WN006 were left at the South Pole in March 2014. Both lamps are designated “long-term” standards and are typically only used during site visits. Both lamps were calibrated by CUCF in August 2013 (see below).

Comparisons of calibrations with the various lamps suggested that the brightness of lamp 200W013 fluctuated greatly over the reporting period. Similar fluctuations have been observed also during the two last seasons. Hence, absolute scans of the lamp were not used for the preparation of solar data.

Calibration history of long-term standards

The long-term standards 200WN005 and 200WN006 were calibrated against lamps 200WN001 and 200WN002 on 8/20/13. Lamps 200WN001 and 200WN002 had in turn been calibrated by Biospherical Instruments in November 2012 against the NIST standard F-616 using a multi-filter transfer radiometer. NIST standard F-616 is traceable to the detector-based scale of irradiance established by NIST in 2000. At the time lamps 200WN001 and 200WN002 were calibrated, they were also compared with the long-term traveling standard 200W017 of the NSF UV monitoring network. The irradiance scales of NIST standard F-616 and lamp 200W017 agreed to within 0.3%.

In early 2020, the chain of calibrations applied to solar data of the NSF and NOAA monitoring networks between 1996 and 2019 was re-evaluated (Bernhard and Stierle, 2020). This analysis suggested that the scale of spectral irradiance of NIST standard F-616 is low compared to the scale of primary standards used before 2013. This bias ranges between -2% at 300 nm, -1% at 375 nm, and less than $\pm 0.5\%$ between 420

and 600 nm. **Version 2 solar data of Volume 29, 30, and 31 were scaled upward accordingly, however, Version 0 data of these volumes remain traceable to the original scale of the primary standard F-616.**

Figure 3.2. shows a comparison of the working standard 200W021 with the long-term standard 200WN006 based on absolute scans performed on 9/9/21, shortly before the commencement of solar measurements at the South Pole. The scales of spectral irradiance of the two lamps agree ideally in the visible range. There is a difference of about 1% in the UV range, which is still within the combined uncertainty of the scales of the two lamps. Unfortunately, scans of lamps M-666 and 200W013 performed on the same day were erratic and a similar comparison with the scan of lamp 200WN006 could not be performed. (Lamp 200WN006 was only used on 9/9/21; hence comparisons with this lamp on other days are not available.) However, results of 200W021 and M-666 for calibration scans performed on 1/15/22 and 2/11/22, respectively, agreed to within 0.5%. Taken together, these results suggest that the calibration scale of solar data of the reporting period, which is based on the scales of lamps 200WN006, 200W021 and M-666, is accurate to within 1%.

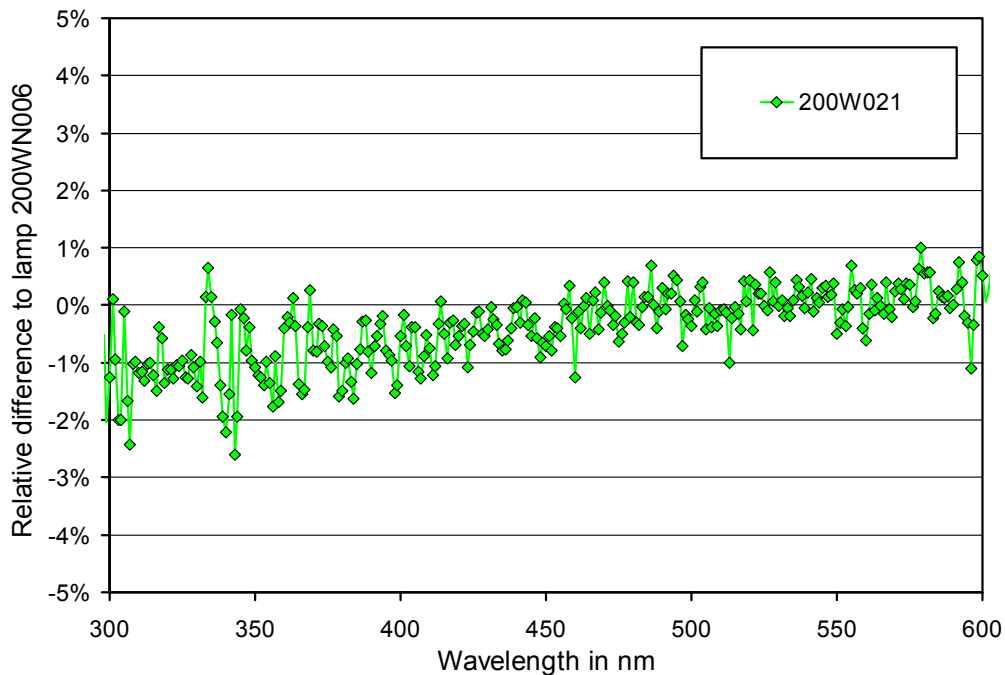


Figure 3.2. Comparison of South Pole working standard 200W021 with long-term standard 200WN006 calculated from calibration scans performed on 9/9/21.

The GUV-541 radiometers was calibrated vicariously against SUV-100 Version 0 data. Calibration factors were established in the same way when data of previous volumes were processed. Calibration factors of the last six years (Volumes 23 –31) agree to within $\pm 1.4\%$ ($\pm 1\sigma$) for all GUV channels, with exception of the drifting 320 nm channel. This result confirms the good consistency of calibrations over time.

3.2. Instrument Stability

The temporal stability of the spectroradiometer’s sensitivity was assessed with (1) bi-weekly calibrations utilizing the on-site standards, (2) daily “response” scans of the internal irradiance reference lamp, (3) comparison with data of the collocated GUV-541 radiometer, and (iv) model calculations, which are part of the “Version 2” data edition (Bernhard et al., 2004).

The internal reference lamp is monitored with a filtered photodiode with sensitivity in the UV-A range, called “TSI”. This photodiode has proven to be very stable over time and its measurements therefore allow to decouple temporal drifts of the internal lamp from changes in the SUV-100’s responsivity. These changes may be caused by variations in monochromator throughput or PMT sensitivity. Figure 3.3 shows changes in TSI readings and PMT currents at 300 and 400 nm, which were derived from the daily scans of the internal lamp during the reporting period. TSI measurements steadily decreased by about 4% during the reporting period, indicating some dimming of the internal reference lamp. PMT currents at 300 and 400 nm also showed a downward trend in response to the change in the lamp’s output but their variability is larger than that of the TSI data. In addition, there is a sudden drop in the current at 300 nm of about 4% on 11/10/21 for no obvious reasons. The change in PMT currents during the last two weeks of the reporting period is also somewhat larger than that of the TSI measurement. The magnitude of these variations is within the normal range observed in previous years. The resulting changes in the instrument’s sensitivity were corrected by adjusting the system’s calibration as described below.

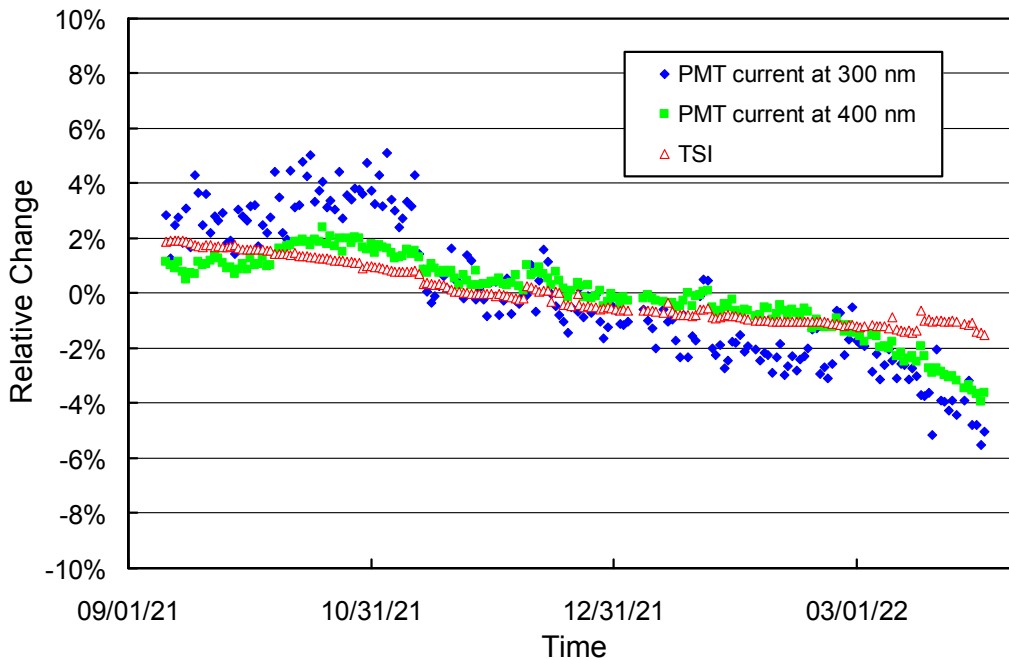


Figure 3.3. Time-series of PMT current at 300 and 400 nm, plus the TSI signal, derived from daily measurements of the SUV-100’s the internal irradiance standard. Data are normalized to the average of the whole period.

A comparison of GUV-541 and SUV-100 measurements allows to detect anomalies in SUV-100 data. Accordingly, Figure 3.4 shows the ratio of GUV-541 (340 nm channel) and SUV-100 measurements. The latter were weighted with the spectral response function of the GUV’s 340 nm channel. The ratio was normalized to its average and should ideally be equal to one at all times. The graphs indicates that GUV and SUV measurements are generally consistent to within $\pm 5\%$. The few outliers can be explained by shading from obstacles (e.g. air sampling masts) that are in the field of view of the instruments. Because GUV and SUV radiometers are not positioned at exactly the same location, the shadows from these obstacles fall on the collectors of the two instruments at different times. Scans affected by shadowing from stacks were flagged in the SUV-100 Version 2 dataset, removed from the GUV dataset, but remain part of the SUV-100 Version 0 dataset. In addition, the ratio has a local maximum on around 11/1/21, at the beginning of Period PID. A similar maximum around this time was also observed historically and is mostly caused by incomplete cosine error correction of GUV and SUV data. (Data used for the plot are based on a preliminary cosine error correction, which is less sophisticated than that used for Version 2 SUV data. For example, it does not take the effect of clouds into account).

The responsivity of the SUV-100 system was stabled to within 5% between the start of the reporting period and 1/14/22 (Period A), and between 1/15/22 and the end of the reporting period (Period B). However, there was a large change in responsivity on 1/15/22 for reasons that could not be identified. In total, ten calibration functions were established to correct for changes in responsibility. Six functions were used for Period A and four for Period B. More information on these calibration periods and subperiods is provided in Table 3.1. Times when the calibration changed are also indicated by vertical lines in Figure 3.4. The ratios of these calibrations functions relative to the function calculated for Period P3 are shown in Figures 3.5.

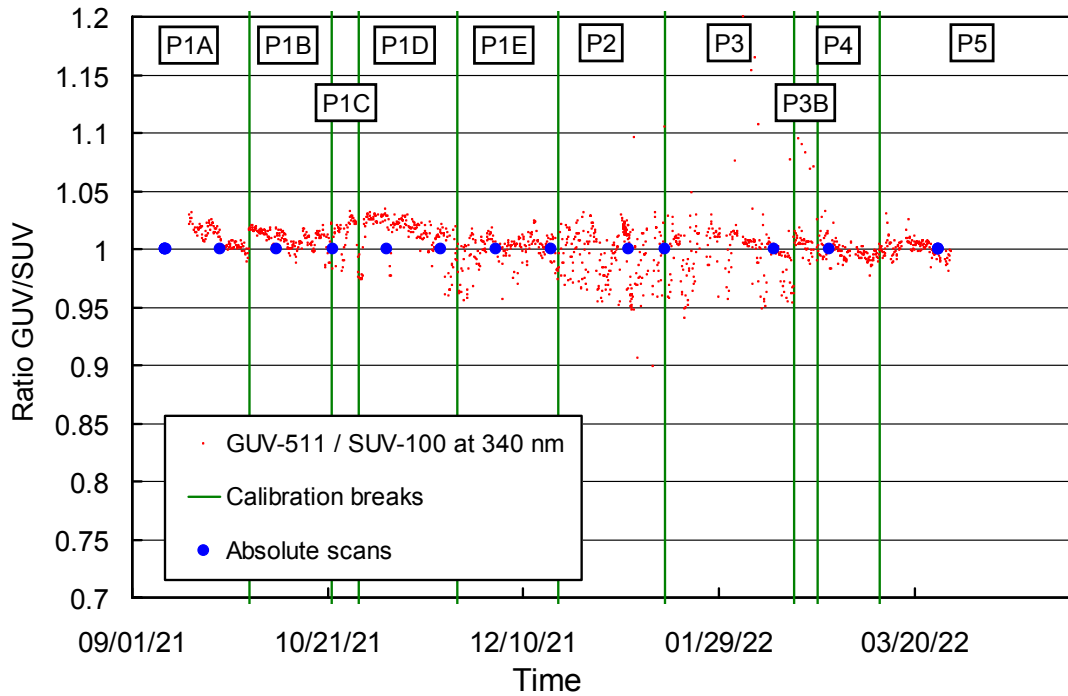


Figure 3.4. Ratio of GUV-541 (S/N 29239) measurements (340 nm channel) with SUV-100 measurements. SUV-100 data were weighted with the spectral response function of this GUV channel. The vertical green lines indicate times when the calibration applied to SUV-100 data was changed (see also Table 3.1).

Table 3.1 Calibration periods for South Pole data of Volume 31.

Period and Subperiod	Period range	Number of absolute scans	Remarks
A: P1A	06/21/21 – 09/30/21	2	Scaled by –1.5% to 2.5%
A: P1B	10/01/21 – 10/21/21	} 2 for subperiods P1B–P1E	Scaled by –1.5% to 2.5%
A: P1C	10/22/21 – 10/28/21		Scaled by –0.6% to 0.7%
A: P1D	10/29/21 – 11/22/21		Scaled by +0.5% to 1.1%
A: P1E	11/23/21 – 12/18/21		Scaled by +1.4% to 2.6%
A: P2	12/19/21 – 01/14/22	1	
B: P3	01/15/22 – 02/16/22	2	
B: P3B	02/17/22 – 02/22/22	0	Average of P3 and P4
B: P4	02/23/22 – 03/10/22	1	
B: P5	03/11/22 – 06/01/22	1	

Because of the instability of lamp 200W013 and some issues with other calibration scans, relatively few calibrations scans were available to establish calibration functions. The network’s standard calibration

scheme for processing of solar data could therefore not be applied as this scheme requires that several calibrations scans are available for each calibration period. Instead, calibrations were either based on the scan with the most reliable lamp (typically 200W021, sometimes also M-666, or a combination of these two lamps), the average of calibrations of adjacent calibration factors, or calibrations scaled with functions that were constructed based on comparisons with measurements of the GUV radiometer. The latter approach assumes that the GUV radiometer was stable over the short periods required for these adjustments. Details of these adjustments are summarized in column “remarks” of Table 3.1. Because the methods used for establishing calibration functions are not ideal, uncertainties of published solar data for some periods are slightly (~2%) larger than typical. However, the agreement of SUV and GUV data that are shown in Figure 3.4 and the good agreement between measurements and data modeled as part of Version 2 data processing confirm that uncertainties of published SUV-100 data remain within acceptable limits.

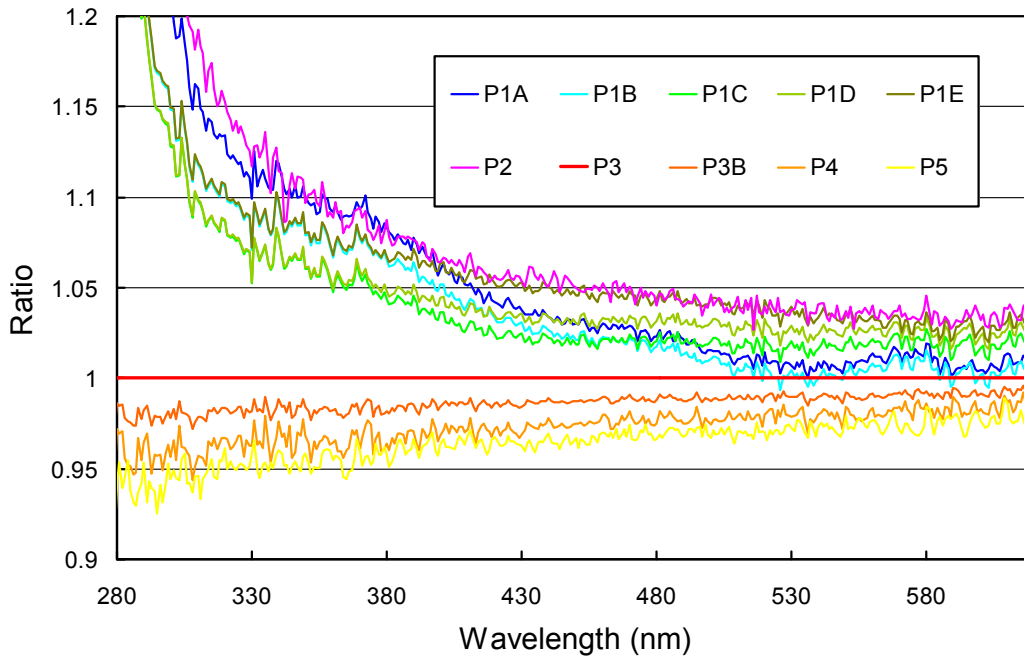


Figure 3.5. Ratios of spectral irradiance assigned to the internal lamp relative to the spectral irradiance of Period P3.

3.3. Wavelength Calibration

The wavelength stability of the system was monitored with the internal mercury lamp. Information from the daily wavelength scans was used to homogenize the data set by correcting day-to-day fluctuations in the wavelength offset. The wavelength-dependent bias of this homogenized dataset and the correct wavelength scale was determined with the Version 2 Fraunhofer line correlation method (Bernhard et al., 2004). The resulting correction function is shown in Figure 3.6.

Figure 3.7 indicates the wavelength accuracy of Version 0 data for five wavelengths in the UV and visible range. The plot was generated by applying the Version 2 Fraunhofer-line correlation method to the corrected data. Residual wavelength shifts are typically smaller than ± 0.10 nm, but there is still a noticeable day-to-day variability. The wavelength accuracy was further improved when processing Version 2 data by breaking the dataset into 90 periods and calculating separate correction functions for each period. Figure 3.8 indicates the wavelength accuracy of Version 2 data. A significant improvement in the wavelength uncertainty can be observed when comparing Figs. 3.7 and 3.8. The standard deviation of the residual wavelength shifts is smaller than 0.038 nm at all wavelengths.

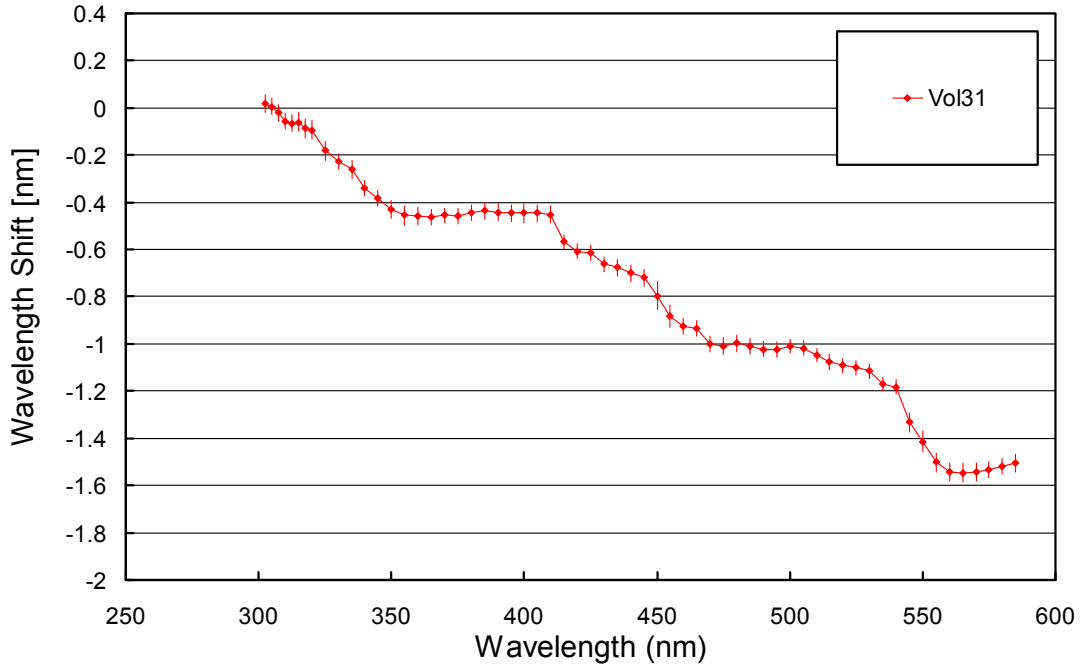


Figure 3.6. Monochromator non-linearity correction functions.

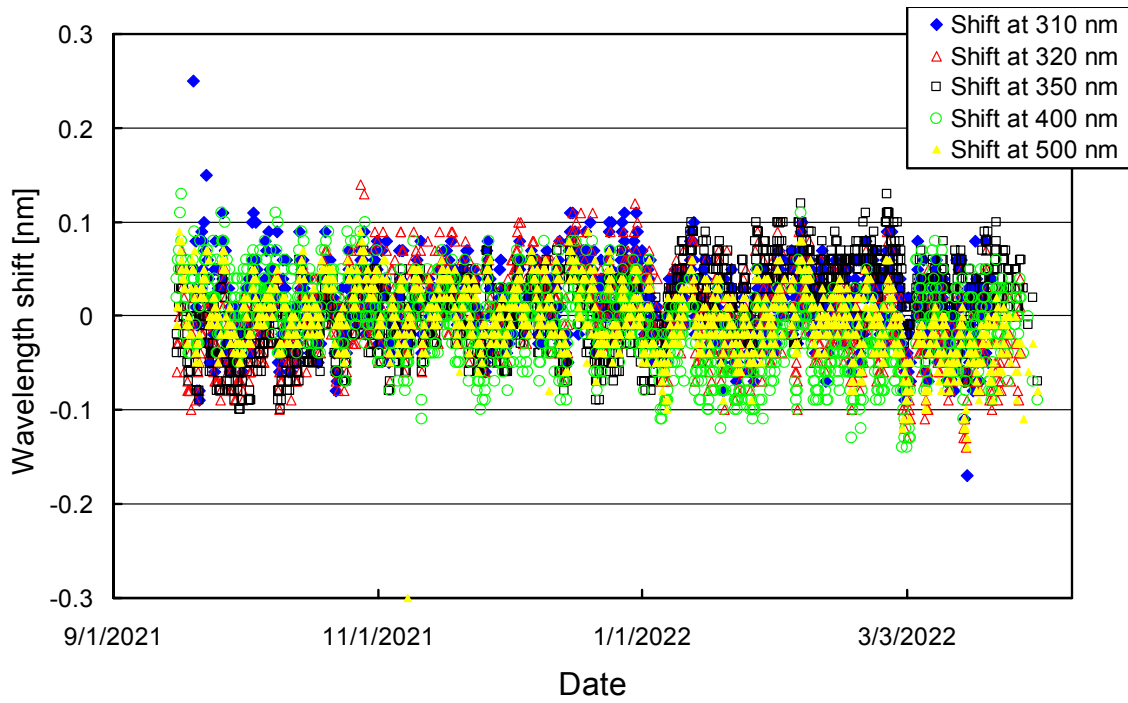


Figure 3.7. Wavelength accuracy check of Version 0 data at five wavelengths by means of Fraunhofer-line correlation.

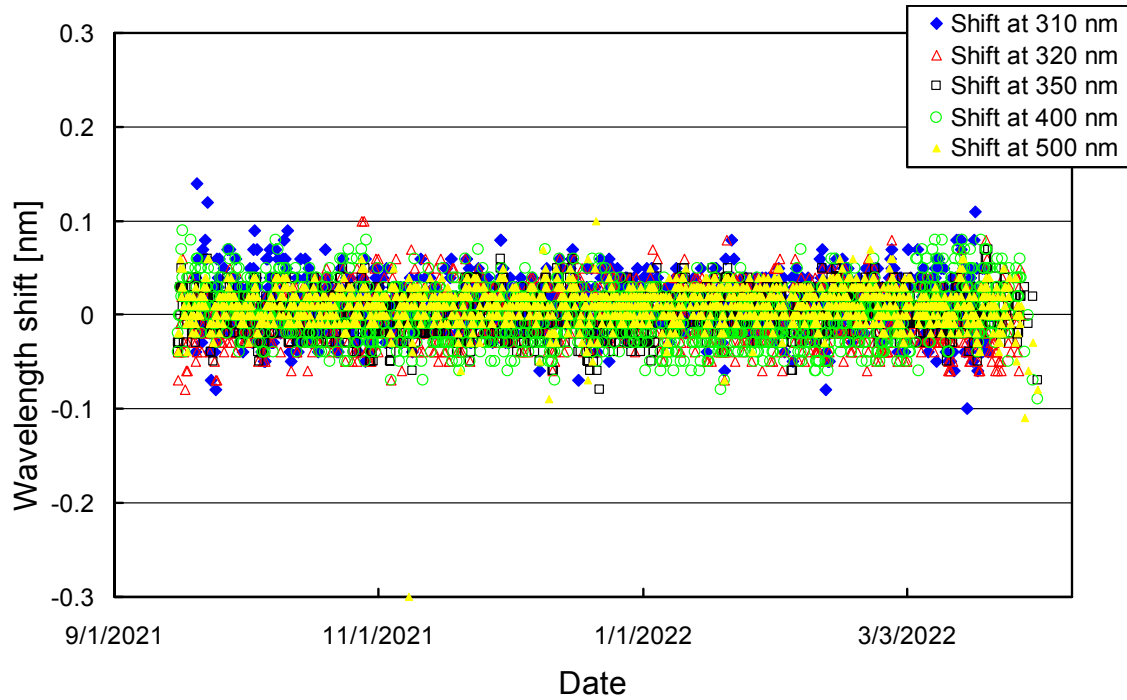


Figure 3.8. Wavelength accuracy check of *Version 2* data at five wavelengths by means of Fraunhofer-line correlation.

References

Bernhard, G., C. R. Booth, and J. C. Ehranjian. (2004). Version 2 data of the National Science Foundation’s Ultraviolet Radiation Monitoring Network: South Pole, *J. Geophys. Res.*, 109, D21207, doi: <https://doi.org/10.1029/2004JD004937>.

Bernhard G. and S. Stierle (2020). Trends of UV Radiation in Antarctica, *Atmosphere*, 11(8), 795, doi: <https://doi.org/10.3390/atmos11080795>.